Dynamic Characterization of a Micro-machining Spindle

ICOMM
2014
No.

Byron Knapp and Dave Arneson

Professional Instruments Company, Hopkins, Minnesota, USA

Abstract

Ultra-precision micro-machining processes such as diamond micro-milling are used to efficiently manufacture optical quality surfaces. These processes require high stiffness spindles with low synchronous and asynchronous error motions throughout the range of desired spindle speeds. This paper describes dynamic testing of a 50,000 RPM micro-machining air bearing spindle with nanometer-lever error motions capable of producing optical quality surfaces.

Keywords: micro-machining, diamond machining, spindle dynamics, run-out

1. Introduction

Diamond machining processes are used to manufacture surfaces with 1-10 nm Ra finish and 0.1-1 µm Pt form error [1]. Furthermore, advanced wafer-level optics require features with highly aspheric, high-NA lenses and lens sag beyond the limitations of etching and step-and-repeat processes [2]. These processes require high-speed spindles for high performance [3] with low error motions for surface quality [4].

Figure 1 shows two examples of micro-milled lens arrays. They are machined using single flute diamond ball end-mills as shown in Figure 2. The diamond end-mill is mounted to the 50,000 RPM air bearing micro-machining spindle discussed in this paper.

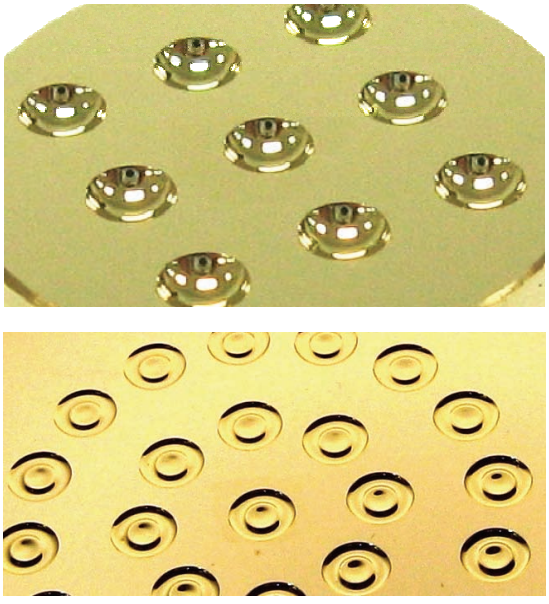

Fig. 1. Examples of micro-milled lens arrays. Photo credit: Moore Nanotechnology Systems.

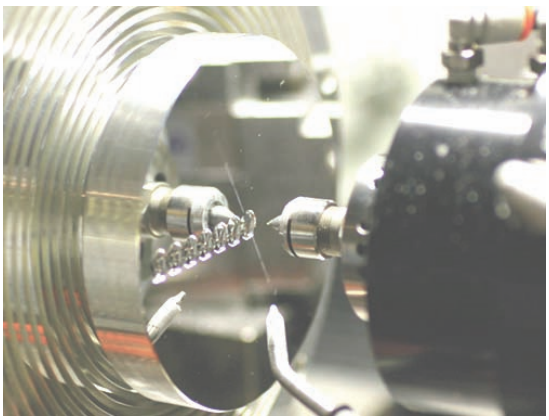

Fig. 2. Milling a lens array with a single flute diamond ball end-mill mounted in an air bearing spindle. Photo credit: II-VI Incorporated.

2. Design

The air bearing spindle used to diamond mill the lens array is shown in Figure 3. It incorporates a “captured thrust” groove compensated air bearing between two radial groove compensated air bearing journals. Air is ported through the stator to annular manifolds that distribute it to radial and thrust bearings. Wide journal bearing spacing provides tilt capacity and stiffness, enabling the use of a smaller diameter thrust and reducing heat generation of the air films. Typically, a trade-off exists between a high speed and a high stiffness spindle design. Tighter clearances will provide higher stiffness but create more heat due to drag and additional motor heat. In this spindle, axial and radial air films are 7 µm and spindle temperature is controlled using integrated water-cooling. The spindle features a 100-line count rotary encoder, a brushless permanent magnet servo motor and provision for balancing.

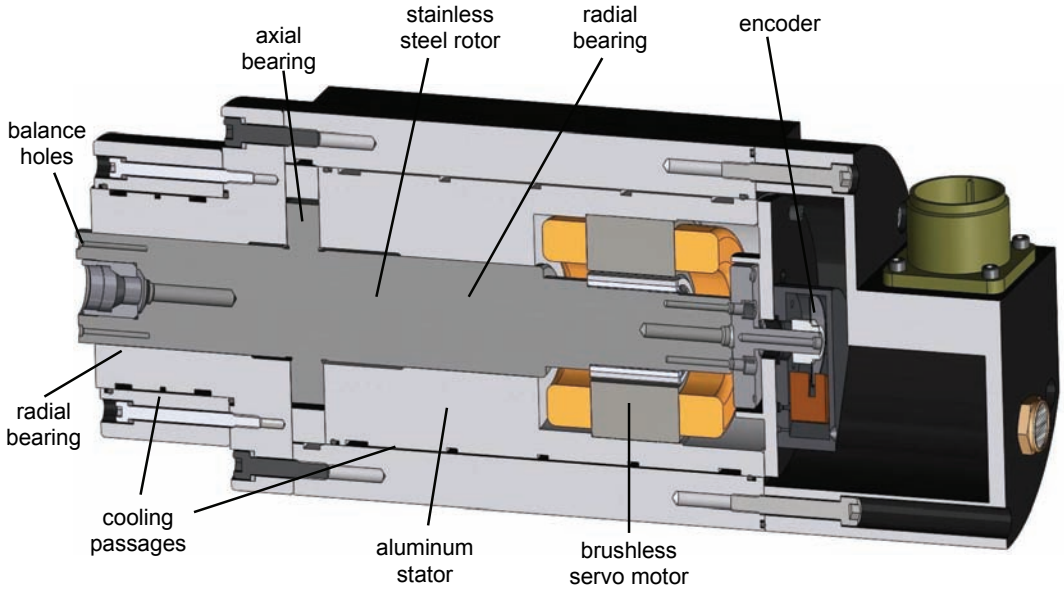

Fig. 3. Sectioned view of the air bearing spindle under test.

3. Dynamic testing

This paper demonstrates a comprehensive approach to dynamic testing, balancing and error motion measurement—three issues that influence surfaces machined with high speed spindles.

3.1. Dynamic response

A modal impact test was performed to determine the dynamic properties of the air bearing spindle. An impact hammer was used to excite the structure and a capacitive sensor is used to measure the response. With an inlet pressure of 0.69 MPa (100 PSI), the first mode of the radial cross-point compliance is 1,160 Hz (see Fig. 4.).

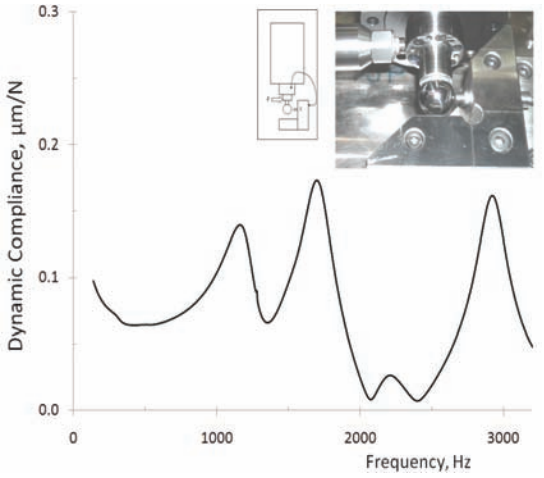

Fig. 4. Radial cross-point compliance. Impacting the spindle nose and measuring the response at the nose.

Surface accuracy is negatively affected when the dominant structural resonance occurs at an integer multiple of the spindle speed [5]. In this case, the first natural frequency (1,160 Hz) is higher than the maximum spindle speed (833 Hz).

3.2. Balancing

Unbalance at high speeds is a major concern in the manufacture of optical-quality freeform surfaces. It is well-documented that unbalance has little or no effect on surface finish in single-point diamond turning [6]. However, it has been shown that first and higher order harmonics can be excited in a machine structure by a rotating unbalance leading to features that are not concentric, flat or round [7].

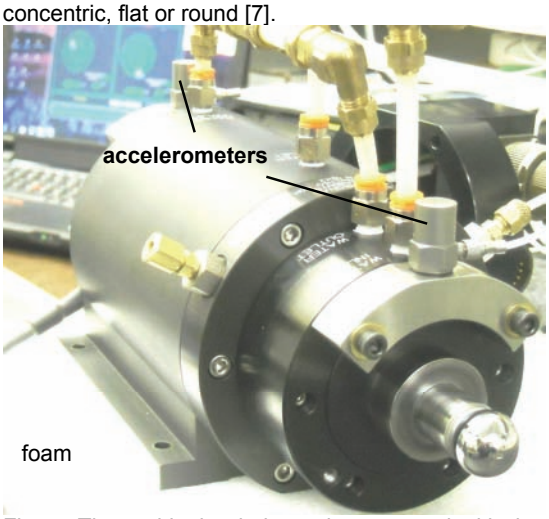

Fig. 5. The residual unbalance is measured with the spindle on foam. Accelerometers are located at the balance planes.

Vibration of a machine structure resulting from a rotating unbalance force or moment may lead to many problems, including fundamental (once-per-revolution) axial motion, higher order harmonic motion, accelerated tool wear, and poor dimensional control with changes in speed.

The setup for balancing the spindle on foam is shown in Figure 5. Accelerometers are mounted as close as possible to the two spindle correction planes. Screws of known weight are used to calibrate the output of the accelerometers. The spindle encoder is used for angular orientation and balancing software calculates the required mass correction. Use of the encoder index eliminates the need for an external fiducial, such as reflective tape, which can negatively influence balance. Weight corrections on the order of micrograms are removed from M3 setscrews at each balance plane. The final result in Figure 6 shows that the balance is better than grade G0.1. This correction is so small that a buffing wheel is all that is needed to remove weight from the setscrew. The unbalance-induced eccentricity shown in Figure 7 is less than 500 nm over the speed range (up to 50,000 RPM).

Fig. 6. Residual unbalance correction in both planes is about 0.5 milligrams. This is better than grade G0.1.

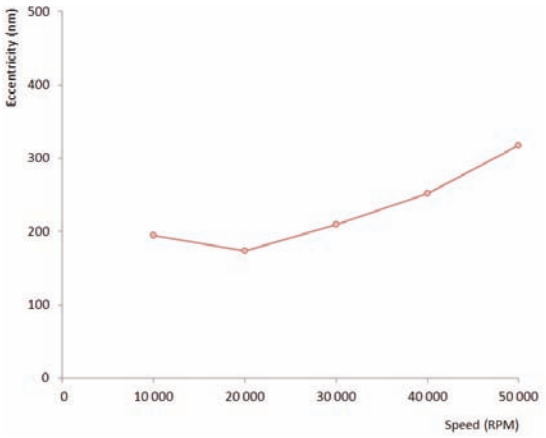

Fig. 7. The unbalance-induced eccentricity is less than 500 nm over the entire speed range.

3.3. Error motion measurement

The ultra-precision air bearing in this work is designed to run up to 50,000 RPM with less than 25 nm total axial and total radial error motions. Accuracy requirements to this level demand rigid test hardware and minimization of external influences.

Error motion tooling shown in Figure 7 features a large granite base with passive air isolation, stiff steel structure with a stiff structural loop between the spindle stator and the sensor mounts. A capacitive sensor (Lion Precision C23-C, 2 V/µm) targets a lapped spherical artifact in the radial and axial directions. The sensor amplifier (Lion Precision CPL290) incorporates a 15 kHz first-order, low-pass analog filter with linear phase response. The data acquisition system (Lion Precision SEA V8.5) is triggered by the 100-line count encoder data channel, providing immunity to synchronization errors caused by speed variation.

Fig. 8. Tooling for radial and axial error motion measurement is designed to minimize structural error motion.

The artifact shown in Figure 9 is a monolithic Ø19 mm flange-mounted ball for maximum stiffness and uniform circular compliance. The 5 nm form error of the ball is not removed from test results. Elements of the structural loop from sensor to artifact are designed to be as stiff as possible.

Fig. 9. Monolithic Ø19 mm flange-mounted ball. The superior stiffness of the screw joint flange-mount and single-piece ball is essential for nanometer-level error motion measurement at high speeds.

Typical error motion polar plots for radial (Fig 10) and axial (Fig 11) error motion at 50,000 RPM are shown. The total radial and axial error motions over the entire speed range are summarized in Figure 12 and Figure 13.

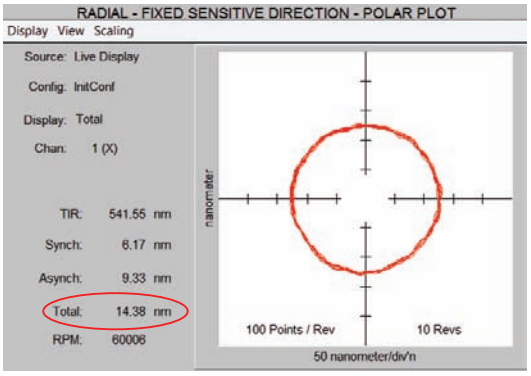

Fig. 10. Radial error motion measurement at 50,000 RPM including artifact out-of-roundness.

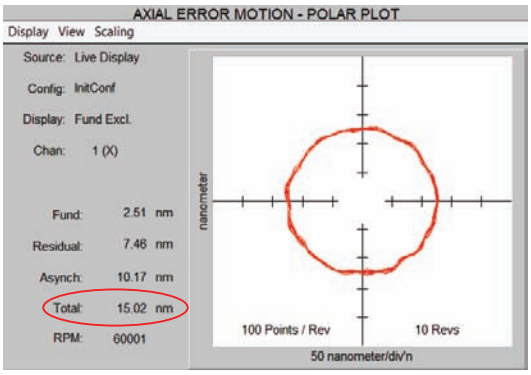

Fig. 11. Axial error motion at 50,000 RPM.

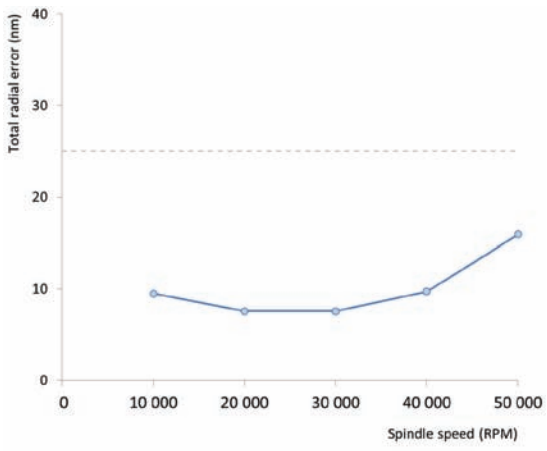

Fig. 12. Summary of total radial error motion at all speeds (including the artifact out-of-roundness).

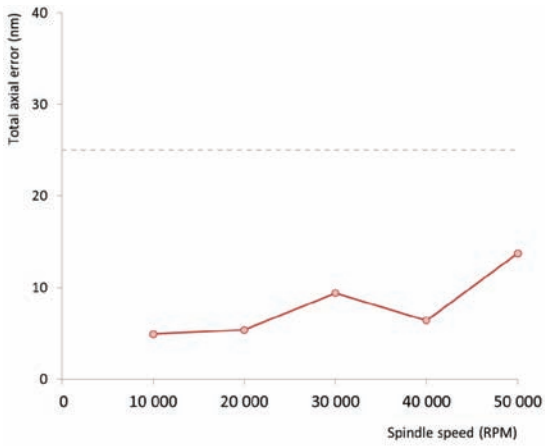

Fig. 13. Summary of total axial error motion at all speeds.

4. Cutting tests

In order to demonstrate the benefits the ultra-precision spindle, micro-milling tests were performed using the 3-axis freeform generator shown in Figure 14. The machine incorporates oil hydrostatic slides and a compact structural loop which result in exceptional stiffness and damping. This enables the advantages of the precision spindle to be fully realized.

A concave asphere was machined in brass with odorless mineral spirits as a coolant. A single flute diamond ball mill is mounted in the air bearing spindle running at 40,000 RPM. The form error and surface finish are shown in Figure 15. The peak-to-valley form error as measured with the Taylor Hobson profilometer is Pt = 97 nm. The surface finish measured with a Zygo white light interferometer is Ra = 1.6 nm.

Fig. 14. Cutting tests performed with the Nanotech 350FG Ultra Precision 3-Axis Freeform Generator. Photo credit: Moore Nanotechnology Systems.

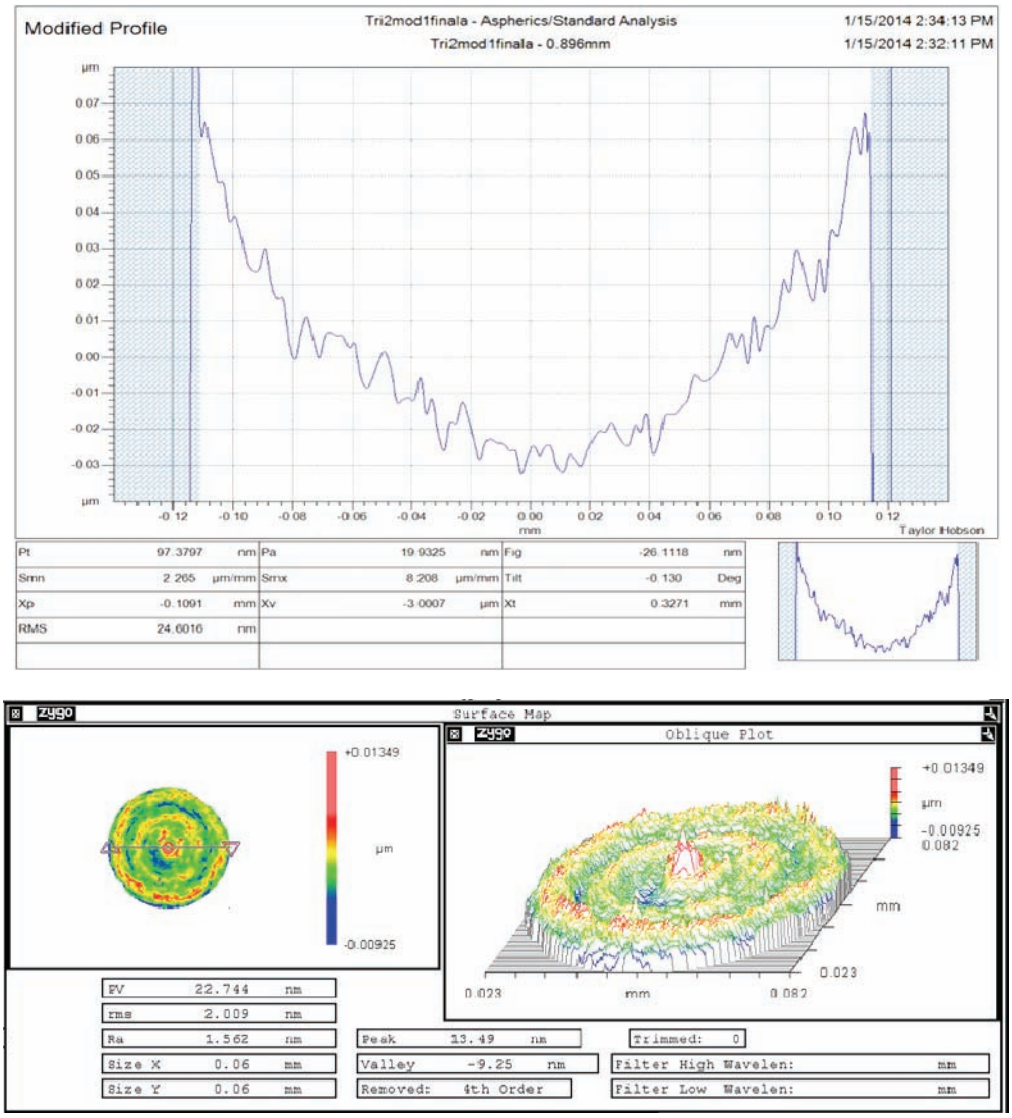

Fig. 15. Form error and surface finish of the cutting tests. Form error is Pt = 97 nm and surface finish is Ra = 1.6 nm. Photo credit: Moore Nanotechnology Systems.

5. Conclusion

Dynamic testing techniques and apparatus required for an ultra-precision high speed micro-milling spindle are described. The cross-point frequency response function indicates that the critical first natural frequency of the spindle is above the maximum spindle speed. Over the entire speed range, the unbalance induced eccentricity for this spindle is shown to be below 0.5 µm as a result of precision balancing and high spindle stiffness. Total axial error motion and total radial error motions for this spindle are less than 16 nm at all speeds. Axial and radial asynchronous errors, critically important for optical quality surfaces, are less than 15 nm at all speeds. Cutting tests of a milled asphere demonstrate form errors better than 100 nm and surface finish better than 2 nm.

References

[1] E Brinksmeier et al., “Micro-machining,” Phil. Trans. R. Soc. A, 2012; 370: 3973-3992.

[2] NCR Holme et al. “Diamond micro-milling for array mastering,” Proc. SPIE 7062, 2008.

[3] FZ Fang et al., “Manufacturing and measurement of freeform optics,” CIRP Annals – Manuf. Tech., 2013; 62: 823-846.

[4] D Dornfeld et al., “Recent advances in mechanical micromachining,” Annals of the CIRP, 2006; 55(2): 745-768.

[5] E Marsh et al., “The effects of spindle dynamics on precision flycutting,” Proc. ASPE Annual Meeting: 2005.

[6] ANSI/ASME B89.3.4-2010. Axes of Rotation; Methods for Specifying and Testing. ASME, 2010.

[7] J. Byran et al., “Spindle Accuracy,” American Machinist, 1967; December: 149-162.